

# MicroRNA-218-5p Promotes Endovascular Trophoblast Differentiation and Spiral Artery Remodeling

Jelena Brkić,<sup>1</sup> Caroline Dunk,<sup>2</sup> Jacob O'Brien,<sup>1</sup> Guodong Fu,<sup>1,2</sup> Lubna Nadeem,<sup>1,2</sup> Yan-ling Wang,<sup>3</sup> David Rosman,<sup>4</sup> Mohamed Salem,<sup>1</sup> Oksana Shynlova,<sup>2,5,8</sup> Issaka Yougbaré,<sup>6,7</sup> Heyu Ni,<sup>6,7,8,9,10</sup> Stephen J. Lye,<sup>2,5,8</sup> and Chun Peng<sup>1,11</sup>

<sup>1</sup>Department of Biology, York University, Toronto, ON M3J 1P3, Canada; <sup>2</sup>Lunenfeld-Tanenbaum Research Institute, Mount Sinai Hospital, Toronto, ON M5T 3H7, Canada; <sup>3</sup>State Key Laboratory of Stem Cell and Reproductive Biology, Institute of Zoology, Chinese Academy of Sciences, Beijing 100101, China; <sup>4</sup>Obstetrics and Gynaecology, Mackenzie Richmond Hill Hospital, Richmond Hill, ON L4C 4Z3, Canada; <sup>5</sup>Department of Obstetrics and Gynecology, University of Toronto, Toronto, ON M5G 1E2, Canada; <sup>6</sup>Toronto Platelet Immunobiology Group and Department of Laboratory Medicine, Keenan Research Centre for Biomedical Science, St. Michael's Hospital, Toronto, ON, Canada, M5B 1W8; <sup>7</sup>Canadian Blood Services, Toronto, ON K1G 4J5, Canada; <sup>8</sup>Department of Physiology, University of Toronto, Toronto, ON M5S 1A8, Canada; <sup>9</sup>Department of Laboratory Medicine and Pathobiology, University of Toronto, Toronto, ON M5S 1A8, Canada; <sup>10</sup>Department of Medicine, University of Toronto, Toronto, ON M5S 1A8, Canada; <sup>11</sup>Centre for Research in Biomolecular Interactions, York University, Toronto, ON M3J 1P3, Canada

**Preeclampsia (PE) is the leading cause of maternal and neonatal morbidity and mortality. Defects in trophoblast invasion, differentiation of endovascular extravillous trophoblasts (enEVTs), and spiral artery remodeling are key factors in PE development. There are no markers clinically available to predict PE, leaving expedited delivery as the only effective therapy. Dysregulation of miRNA in clinical tissues and maternal circulation have opened a new avenue for biomarker discovery. In this study, we investigated the role of miR-218-5p in PE development. miR-218-5p was highly expressed in EVT cells and significantly downregulated in PE placentas. Using first-trimester trophoblast cell lines and human placental explants, we found that miR-218-5p overexpression promoted, whereas anti-miR-218-5p suppressed, trophoblast invasion, EVT outgrowth, and enEVT differentiation. Furthermore, miR-218-5p accelerated spiral artery remodeling in a decidua-placenta co-culture. The effect of miR-218-5p was mediated by the suppression of transforming growth factor (TGF)- $\beta$ 2 signaling. Silencing of *TGFB2* mimicked, whereas treatment with TGF- $\beta$ 2 partially reversed, the effects of miR-218-5p. Taken together, these findings demonstrate that miR-218-5p promotes trophoblast invasion and enEVT differentiation through a novel miR-218-5p-TGF- $\beta$ 2 pathway. This study elucidates the role of an miRNA in enEVT differentiation and spiral artery remodeling and suggests that downregulation of miR-218-5p contributes to PE development.**

## INTRODUCTION

Preeclampsia (PE) is the leading and direct cause of maternal and neonatal morbidity and mortality.<sup>1</sup> Currently there are no predictive methods clinically available, and the only effective treatment for PE is delivery of the placenta and baby, often preterm, elevating the risk of fetal complications.<sup>2</sup> The risk to the mother does not end with the

pregnancy; a relationship of developing PE during pregnancy to future cardiovascular and metabolic diseases has been well established.<sup>3,4</sup> Furthermore, numerous studies report that babies born to PE mothers have a significantly greater risk of developing cardiovascular diseases later in life.<sup>5,6</sup>

The pathogenesis of PE is not well understood; however, it is recognized that the placenta is the origin. A successful pregnancy depends on healthy function of the placenta, which requires the precise and coordinated differentiation of cytotrophoblast cells (CTBs) into interstitial extravillous trophoblasts (iEVTs) that invade the decidua. A subset of EVT cells further differentiates into endovascular EVT cells (enEVTs) that invade the maternal uterine spiral arteries during vascular transformation. Remodeling of the uterine spiral arteries into large dilated sinusoids is essential for adequate perfusion of the placenta to support and sustain the increasing requirements of the growing fetus.<sup>7</sup> The molecular mechanisms governing the development of these two distinct EVT subtypes are critical for elucidating the etiology of PE.<sup>8</sup> It has been suggested that shallow EVT invasion into the decidua, along with poor enEVT-mediated remodeling of spiral arteries, is a major cause of PE. This leads to inadequate blood flow to the placenta, resulting in oxidative stress, reperfusion injuries, and systemic maternal endothelial dysfunction.<sup>9</sup>

MicroRNAs (miRNAs) are small non-coding RNAs that regulate gene expression and play important roles in many developmental and physiological processes, including placenta development and

Received 28 December 2017; accepted 3 July 2018;  
<https://doi.org/10.1016/j.ymthe.2018.07.009>

**Correspondence:** Chun Peng, Department of Biology, York University, 4700 Keele Street, Toronto, ON M3J 1P3, Canada.

**E-mail:** [cpeng@yorku.ca](mailto:cpeng@yorku.ca)



function.<sup>10–12</sup> To date, no miRNAs have been implicated in the specific process of enEVT differentiation and spiral artery remodeling.<sup>13</sup> miR-218-5p is processed from two precursor genes, *MIR218-1* and *MIR218-2*, located in introns of *SLIT2* and *SLIT3*, respectively. The Slit-Robo pathway is well known for its role in neuronal and vascular development.<sup>14–18</sup> This pathway is downregulated in PE placentas<sup>19</sup> and has been suggested to regulate angiogenesis in the placental bed.<sup>20,21</sup> Interestingly, a recent study of human ectopic pregnancies reported that migratory EVT and actively remodeling enEVTs are both strongly positive for *SLIT2*.<sup>22</sup> miR-218-5p is expressed in the human placenta, and its levels are also downregulated in PE placental tissues.<sup>23,24</sup> However, the functional role and mechanism of miR-218-5p in the placenta has not been reported.

The transforming growth factor  $\beta$  (TGF- $\beta$ ) family is a large group of growth factors that play fundamental roles in many cellular processes, such as cellular proliferation, differentiation, apoptosis, and angiogenesis.<sup>25</sup> They signal through a complex of type I and type II serine and/or threonine receptors and a family of intracellular signaling molecules, SMADs.<sup>26</sup> Many studies, including those from our lab, have demonstrated that the TGF- $\beta$  signaling pathway plays important roles in regulating trophoblast survival, proliferation, and invasion.<sup>27–29</sup>

In this study, we investigated the expression and function of miR-218-5p in the human placenta. We confirmed that miR-218-5p was decreased in PE placental tissues, as shown previously,<sup>23,24</sup> and report that the expression of miR-218-5p is upregulated at the initiation of the invasive EVT pathway. We demonstrate that miR-218-5p promotes invasion and enEVT differentiation and accelerates the spiral artery remodeling process. We also provide evidence that *TGFB2* is a target of miR-218-5p. Our study reveals a novel miR-218-5p-mediated mechanism regulating enEVT differentiation that may contribute to the uteroplacental pathology associated with PE.

## RESULTS

### Expression of miR-218-5p in Placentas from Healthy and PE Pregnancies

miR-218-5p is a highly conserved miRNA; a comparison across several hemochorial placenta species showed complete conservation of the entire 21-nt sequence (Figure S1A). To determine the expression level of miR-218-5p in the placenta, we first compared its levels in PE placentas and gestational age-matched controls. PE samples collected from either the basal or chorionic plate of the placenta both showed a significant decrease in miR-218-5p levels compared with controls (Figure 1A). Similarly, miR-218-5p levels were also significantly lower in a second set of clinical samples from Mount Sinai Hospital compared with healthy term controls (Figure S1B). In placentas across gestation, miR-218-5p was detected, and a significantly higher level was observed in the second trimester (Figure 1B). A closer investigation of the first-trimester anchoring villi showed that miR-218-5p levels were significantly upregulated in the EVT and tips of villi starting at 8+ and 9+ weeks of gestation, respectively,

whereas miR-218-5p levels in the branch portion of the villi remained consistent throughout the 6- to 11-week period (Figure 1C).

### Overexpression of miR-218 Induces Differentiation toward the enEVT Pathway

To investigate the role of miR-218-5p in placental development, we generated a miR-218-1-overexpressing cell line. The miR-218-1 stem-loop sequence was cloned into the miRNASelect pEGP-miR expression vector (Figure S1C). The construct was transfected into an immortalized first-trimester trophoblast cell line, HTR8/SVneo, which has been used extensively as an EVT model.<sup>30</sup> Subsequently, positive clones were selected with puromycin treatment. A clone that had 6-fold higher miR-218-5p expression over a control clone that expresses only the empty vector (EV) (Figure 1D) was chosen for functional studies. The miR-218-1-overexpressing cells displayed clear morphological differences compared with control cells. They were smaller and spindle-shaped and grew in a more diffuse mesenchymal pattern (Figure 1E). The rate of cell growth of miR-218-1-overexpressing cells was significantly slower compared with the EV (Figure 1F). Confocal microscopy revealed a vastly more disorganized microtubule network with asymmetric distribution in miR-218-1-overexpressing cells compared with control cells (Figure 1G).

### miR-218-5p Upregulates Key Markers of Invasion and enEVT Differentiation

To determine which genes are regulated by miR-218-1, a cDNA microarray was used. Interestingly, several enEVT markers and genes associated with trophoblast invasion and enEVT differentiation were among the top genes upregulated by miR-218-1 (Figure 2A). Enriched gene ontology terms included negative regulation of proliferation, cellular migration, chemotaxis, and vascular development (Figure S2). mRNAs for several key markers were validated by qRT-PCR. Matrix metalloproteinase-1 (MMP-1), integrin  $\alpha$  1 (ITGA1), platelet and endothelial cell adhesion molecule 1 (PECAM1), Cadherin 5 (CDH5, also known as vascular endothelial (VE)-Cadherin), endothelial cell-specific chemotaxis regulator (ECSCR), interleukin-8 (IL-8), interleukin-1b (IL-1B), and chemokine C-X-C motif ligand 1 (CXCL1) were all significantly upregulated in miR-218-1-overexpressing cells (Figure 2B). Similarly, in primary first-trimester anchoring villi, we found that treatment with an miR-218-5p mimic upregulated MMP-1, ITGA1, PECAM1, CDH5, IL8, and IL1B mRNA levels compared with a non-targeting control (NC) (Figure 2C). In contrast, inhibition of endogenous miR-218-5p by anti-miR-218-5p (Figure 2D) downregulated some of the markers compared with the anti-scramble control (Figure 2E). In addition, the conditioned medium from the miR-218-5p-treated group showed significant changes in secretory proteins important in the establishment of the fetoplacental interface. Specifically, IL-8, CXCL1, IL-6, chemokine C-C motif ligand 2 (CCL2), CXCL16, C-X3-C motif chemokine ligand 1 (CX3CL1), and macrophage migration inhibitory factor (MIF) were upregulated in the conditioned medium of miR-218-5p-treated placental explants, whereas soluble endoglin (sEng) was significantly downregulated in miR-218-5p conditioned medium (Figure S3).

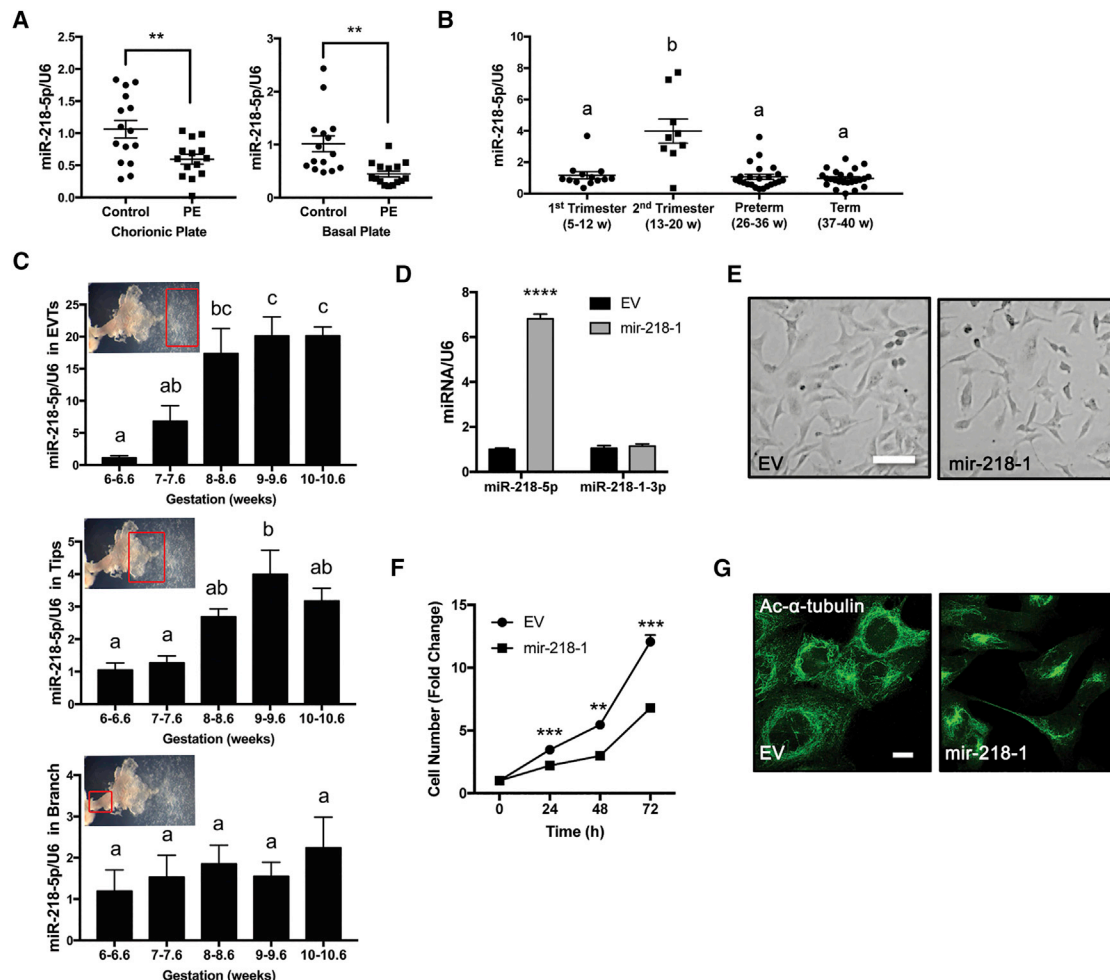


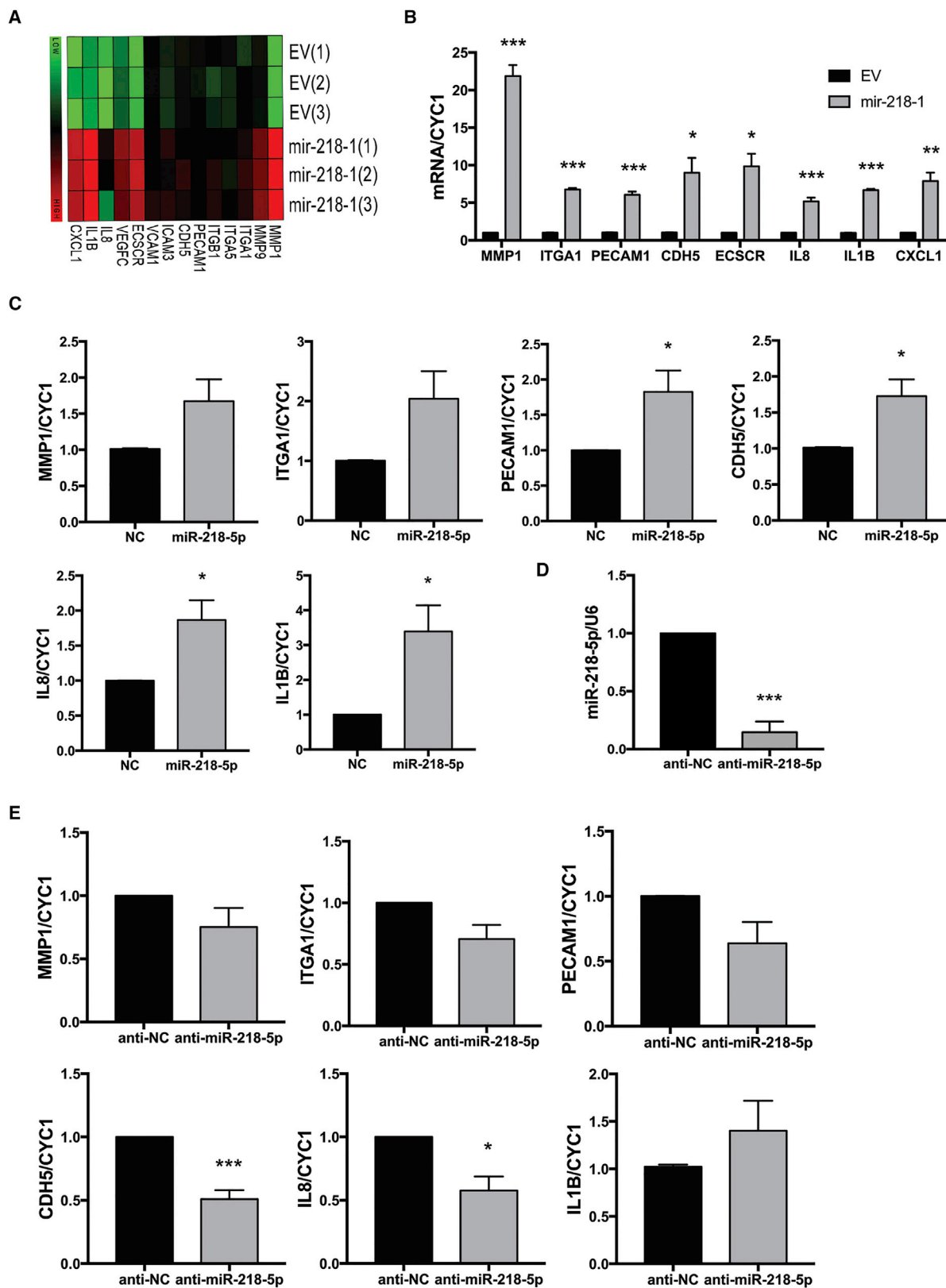
**Figure 1. Expression Pattern of miR-218-5p in Human Healthy and PE Placentas**

(A) miR-218-5p expression in normal and PE placentas. PE and healthy term placentas between 35 and 39 weeks of gestation were collected from the basal and chorionic plates ( $n = 15$  placentas). miR-218-5p was downregulated in PE placentas compared with the control. (B) miR-218-5p levels in placentas across gestation ( $n = 9-24$  placentas). An increase ( $p < 0.0001$ ) in miR-218-5p levels during the second trimester was observed compared with all other gestational periods. Different letters above bars denote statistical significance. (C) miR-218-5p expression in different regions of anchoring villi during early pregnancy. Placental samples were obtained from elective terminations from 6–10.6 weeks gestation, dissected into EVT (top), tips (center), and branches (bottom), and measured for miR-218-5p levels. Different letters above bars denote statistical significance ( $n = 3-4$  placentas). An increase in miR-218-5p was observed from 8 and 9 weeks in EVT and tips, respectively. No difference in miR-218-5p expression was observed in villi branches. (D) Confirmation of miR-218-5p overexpression in HTR-8/SVneo cells stably transfected with mir-218-1 versus cells transfected with empty vector (EV). (E) Morphological examination of stable mir-218-1 and control cells seeded in equal numbers showed that mir-218-1 cells were smaller and spindle-shaped, with less cell-cell contact compared with EV cells. Scale bar, 100  $\mu\text{m}$ . (F) Cell proliferation assays showed mir-218-1-overexpressing cells grew slower than EV cells. (G) Immunofluorescence staining of acetylated  $\alpha$ -tubulin. mir-218-1 cells displayed a more disorganized microtubule network and asymmetric organization. Scale bar, 10  $\mu\text{m}$ . All cell data are representative of three independent experiments. Statistical analysis was performed using (A) unpaired two-tailed Student's *t* test with Welch's correction, (B and C) one-way ANOVA with Tukey's test, or (D and F) multiple *t* tests. \*\* $p < 0.01$ , \*\*\* $p < 0.001$ , \*\*\*\* $p < 0.0001$ . Error bars represent SEM.

### miR-218-5p Promotes First-Trimester Trophoblast Migration and Invasion

Since mir-218-1 upregulated enEVT markers and genes involved in invasion, we assessed the migratory and invasive behavior of mir-218-1-overexpressing cells using transwell assays. As expected, mir-218-1 overexpression significantly increased cell migration (Figure 3A) and invasion (Figure 3B), and the invasion-promoting effect of mir-218-1 was reversed by anti-miR-218-5p (Figure S4A). Simi-

larly, transient transfection of miR-218-5p significantly increased cell migration (Figure 3C) and invasion (Figure 3D), whereas anti-miR-218-5p had the opposite effects (Figures S4E and S4F). In a more recently established immortalized first-trimester trophoblast cell line, Swan71, miR-218-5p also enhanced invasion (Figure S4B). miR-218-5p has been reported to inhibit cancer cell invasion;<sup>31-33</sup> we therefore repeated the transwell invasion assay in an ovarian cancer cell line, ES-2. Similar to studies of other cancer cells, miR-218-5p



(legend on next page)

decreased invasion compared with the control (Figure S4C). To further investigate the invasive and migratory effect of miR-218-5p, first-trimester placental explants were treated with controls, miR-218-5p, or anti-miR-218-5p oligos. We found that miR-218-5p significantly promoted the outgrowth of EVT's (Figure 3G), whereas anti-miR-218-5p significantly impeded this process (Figure 3H). Neither miR-218-5p (Figure 3G) nor anti-miR-218-5p (Figure 3H) had significant effects on cytotoxicity, as revealed by lactate dehydrogenase (LDH) assays.

### miR-218-5p Accelerates Spiral Artery Remodeling

To further confirm that miR-218-5p promotes enEVT differentiation, we investigated the angiogenic potential of mir-218-1 stable cells using an *in vitro* endothelium-like network formation assay. We showed that the mir-218-1-overexpressing cells formed more richly branched and extensive networks with a significantly longer total network length compared with control cells (Figure 4A). Conversely, transfection of parental HTR8/SVneo cells with anti-miR-218-5p significantly reduced their network-forming ability (Figure 4B). To determine how overexpression of mir-218-1 in trophoblasts affects their ability to interact with endothelial cells, we co-cultured control or mir-218-1 stable cells with human umbilical vein endothelial cells (HUVECs) at a one-to-one ratio. To differentiate the two cell types, staining with CellTracker green and red dye, respectively, was done prior to seeding (Figure S5). mir-218-1-HUVEC co-culture had a significantly larger total network length than EV-HUVEC co-culture (Figure 4C, left). Interestingly, in co-culture with control cells, HUVECs formed intact tubes. However, in co-culture with mir-218-1-overexpressing cells, trophoblasts displaced the HUVECs to form network branches (Figure 4C, right), suggesting that mir-218-1 enhances the trophoblasts' ability to displace endothelial cells in the network.

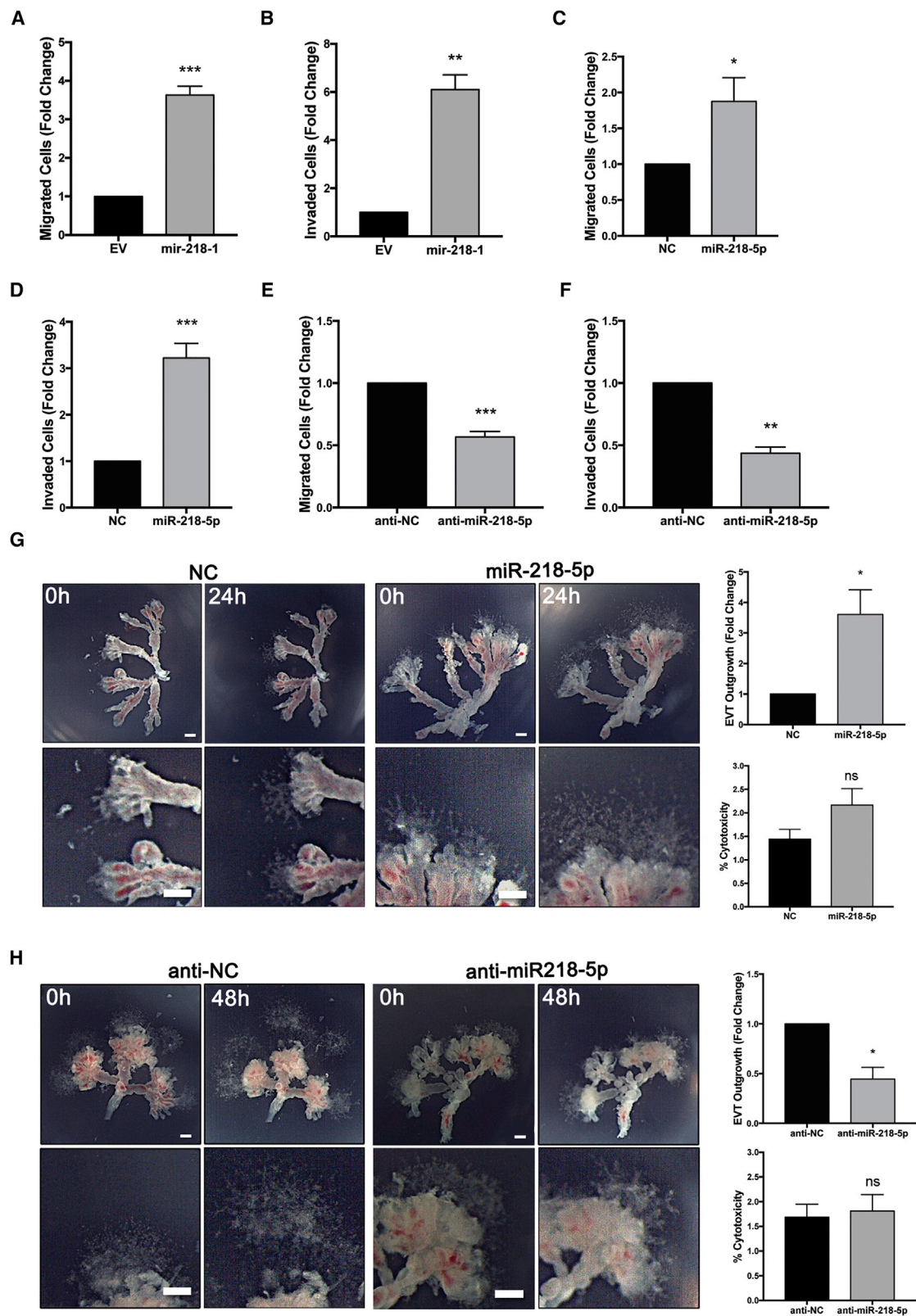
A major function of enEVTs is to replace the endothelial cells lining uterine spiral arteries through vascular remodeling.<sup>34</sup> To examine the role of miR-218-5p in this process, we used a placenta-decidual explant co-culture system previously shown to mirror first-trimester decidual vascular transformation.<sup>35</sup> Placental explants with intact EVT columns were incubated for 24 hr with control or miR-218-5p mimics prior to placement onto the decidual epithelial surface (Figure S6). A decidual-alone culture was used to confirm that there was no sign of trophoblast invasion and spiral artery remodeling *in utero* before the setup of co-culture. As shown in Figures 5A–5E,

the decidual tissue cultured without placental explants was negative for the trophoblast (epithelial) marker cyokeratin-7 (CK-7) and the EVT marker histocompatibility antigen, class I, G (HLA-G) (Figures 5A and 5B). As expected, in non-invaded tissues, decidual controls displayed tight, un-remodeled arterioles that stained positive for the smooth muscle marker smooth muscle actin (SMA) and the endothelial cell marker PECAM1 (Figures 5C and 5D). Leukocytes, positive for lymphocyte common antigen (CD45), were spread evenly throughout the tissue and were not associated with any observed vessels (Figure 5E). In placental-decidual co-cultures pre-treated with NC, the placenta had a large EVT-anchoring column, as shown by CK-7- and HLA-G-positive staining (Figures 5F and 5G). EVT cells were seen invading the lumen of a cross-sectioned arteriole at the proximal end (black arrowheads, Figures 5F and 5G) that displayed a complete loss of smooth muscle cells and nearly all endothelial cells (Figures 5H and 5I, magnified areas). The distal portion of the arteriole (red arrowheads) showed an early "active phase" of vascular transformation with a residual smooth muscle layer (Figure 5H) and an intact endothelial cell layer with signs of endothelial cell swelling (Figure 5I). These changes occurred prior to the presence of trophoblasts and were associated with infiltration of CD45-positive leukocytes in the vessel wall (Figure 5J). In placenta-decidual co-cultures pre-treated with miR-218-5p, an accelerated process of vessel remodeling was evident. The placenta tissue transfected with miR-218-5p mimics displayed large EVT columns positive for both CK-7 and HLA-G (Figures 5K and 5L). Although CK-7 positive EVT's were visible in the proximal portion of the vessel (black arrowheads), they were also present in large numbers in the distal part of the vessel (red arrowheads), where they were seen lining the walls and interacting in the lumen (Figure 5K). The HLA-G marker was lightly positive in the deep invaded trophoblasts (Figure 5L). Nearly all vascular smooth muscle cells were lost, as shown by the lack of SMA staining (Figure 5M). Likewise, the endothelial cell marker PECAM1 was only observed in a few cells lining the vessel wall (Figure 5N, arrowheads). Interestingly, the EVT's in the placental column and distal portion of the vessel were weakly stained for PECAM1 (Figure 5N asterisks). Compared with the NC-pretreated co-culture, there was also a greater extent of leukocyte recruitment to the site of vascular remodeling, with higher numbers of leukocytes directly associating with the wall and in the lumen of the transformed vessel of the miR-218-5p co-cultures (Figure 5O). Similar results were obtained from two additional placenta-decidual co-cultures (Figures S7A

### Figure 2. miR-218-5p Increases the Expression of Key Markers of Trophoblast Invasion and Endovascular Trophoblast Differentiation

(A) Gene expression profiling in EV and mir-218-1 stable cells by cDNA microarray. Several markers of trophoblast differentiation and genes involved in invasion were greatly upregulated in mir-218-1 cells. (B) Validation of genes regulated by mir-218-1. All markers were significantly upregulated in mir-218-1 cells ( $n = 3$  experiments). (C) Regulation of gene expression by miR-218-5p in first-trimester placental explants. Placental tissues were dissected to enrich extravillous trophoblast (EVT) columns and treated with miR-218-5p or a scramble non-targeting control (NC) for 48 hr. miR-218-5p significantly upregulated PECAM1, CDH5, IL-8, and IL-1B mRNA levels versus NC ( $n = 6$  placentas). (D) Anti-miR-218-5p inhibits endogenous miR-218-5p in placental explants. Placental tissues were incubated with anti-miR-218-5p for 48 hr, and miR-218-5p levels were measured ( $n = 6$  placentas). miR-218-5p was downregulated by anti-miR-218-5p. (E) Anti-miR-218-5p downregulated marker gene expression. The RNA samples described in (D) were used for real-time qPCR. Although most markers measured showed a trend of decrease, only CDH5 and IL-8 were significant. Statistical analysis was performed by (B) multiple  $t$  tests ( $\alpha = 0.05$ ) corrected for multiple comparisons with the Holm-Sidak method and (C and D) Welch's  $t$  test ( $p < 0.05$ , 95% confidence interval [CI]) using GraphPad Prism. \* $p < 0.05$ , \*\* $p < 0.01$ , \*\*\* $p < 0.001$ . Error bars represent SEM.





(legend on next page)

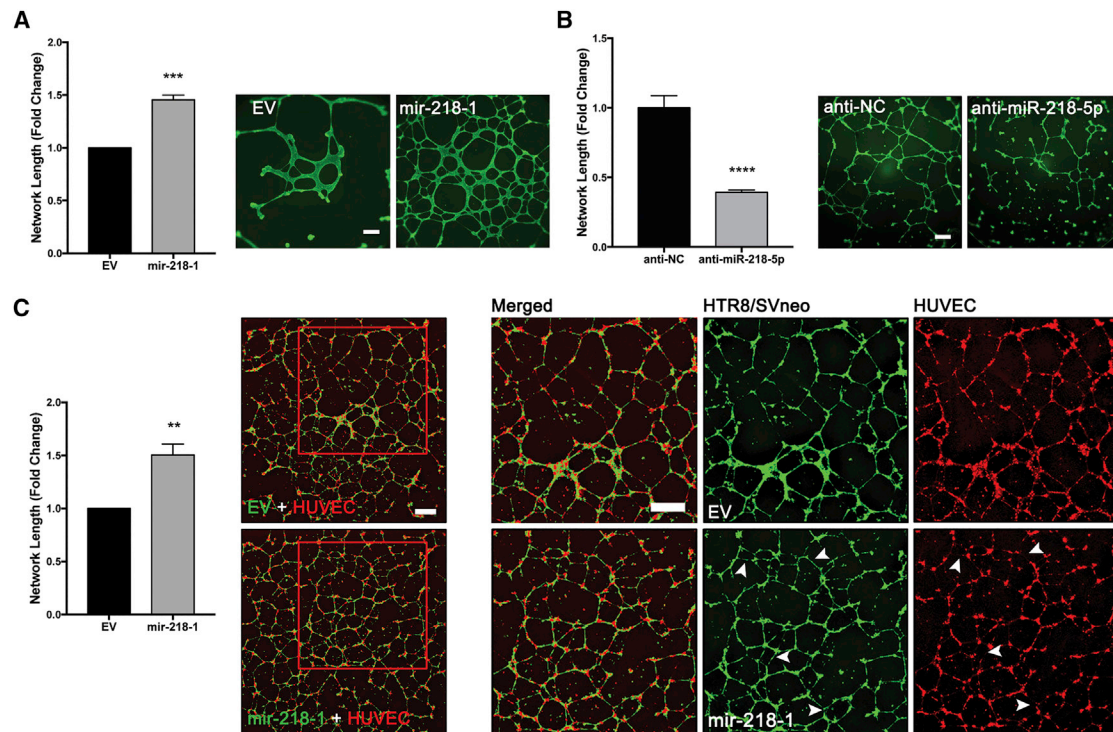


**Figure 4. Overexpression of mir-218-1 Promotes Endothelium-like Network Formation**

(A) mir-218-1 enhances network formation. Control and mir-218-1 stable cells were seeded on Matrigel-coated wells, and network formation was assessed 18 hr after seeding. mir-218-1 cells displayed an increased ability to align into network structures compared with control cells (n = 3 experiments). A representative image is shown. (B) Anti-miR-218-5p inhibits network formation. HTR8/SVneo cells were transiently transfected with anti-miR-218-5p, and network formation assays were performed. Compared with an NC oligo (anti-NC), cells transfected with anti-miR-218-5p showed a decreased ability to form network structures (n = 3). One representative experiment is shown. (C) mir-218-1 stimulates network formation in a co-culture of trophoblasts and HUVECs. Control (EV) or mir-218-1 stable trophoblasts (green) were seeded on Matrigel at a one-to-one ratio with HUVECs (red), and cells were allowed to co-localize and form networks for 18 hr. mir-218-1-HUVEC co-culture showed a more complex network with a larger total length (n = 3). Examination of networks formed on the left showed that, in co-culture with control (EV) trophoblasts, HUVECs formed intact branches. However, in co-culture with mir-218-1-overexpressing cells, the networks formed by HUVECs were not intact (white arrowheads). Representative images are shown. \*\*p < 0.01, \*\*\*p < 0.001, \*\*\*\*p < 0.0001. Error bars represent SEM. Scale bars, 500 μm.

and S7B). Quantification of remodeling vessels revealed that pre-treatment with miR-218-5p led to a doubling of the depth of trophoblast invasion and vascular transformation in comparison with the control (Figure 5P).

**mir-218-5p Promotes Trophoblast Invasion and Differentiation into enEVTs through Suppression of TGF-β2 Signaling**

TGFB2 mRNA contains a predicted binding site for miR-218-5p (Figure S8A), and, therefore, a luciferase reporter containing the TGFB2

3' UTR bracketing the predicted miR-218-5p binding site was generated (Figure S8B). Luciferase assays revealed that miR-218-5p significantly downregulated luciferase activity in the TGFB2 3' UTR reporter (Figure 6A). In addition, TGFB2 mRNA (Figure 6B) and secretion of TGFB2 protein (Figure 6C) were also lower in mir-218-1 cells than in control cells. In contrast to the increased level of miR-218-5p in EVT from mid- to late first trimester, TGFB2 immunoreactivity in the EVT population decreased from 7 to 17 weeks of gestation (Figure S9). Using a SMAD-reporter construct, we found

**Figure 3. miR-218-5p Promotes Trophoblast Invasion, Migration, and EVT Outgrowth**

(A–F) Cells were seeded on transwells without and with Matrigel to assess cell migration or invasion, respectively. Stable transfection of mir-218-1 increased cell migration (A) and invasion (B) compared with control cells transfected with EV. Transient transfection of the miR-218-5p mimics also promoted cell migration (C) and invasion (D) compared with NC. Conversely, anti-miR-218-5p significantly decreased the migratory (E) and invasive (F) ability of the cells compared with controls. The results presented in (A)–(F) are data pooled from a minimum of three independent experiments. (G) Explants from first-trimester placentas were placed on Matrigel and treated with miR-218-5p or control (200 nM) for 24 hr. EVT outgrowth was measured at the time of treatment (0 hr) and at termination of the experiment (24 hr). An increase in EVT outgrowth was observed in miR-218-5p-treated tissues. (H) Explant tissues were treated with anti-miR-218-5p or the control (200 nM) for 48 hr. A decrease in EVT outgrowth was observed with anti-miR-218-5p treatment. Neither miR-218-5p (G) nor anti-miR-218-5p (H) had significant effects on cytotoxicity. Representative images are shown, and bar graphs present data from four experiments with unique placentas. \*p < 0.05, \*\*p < 0.01, \*\*\*p < 0.001. Error bars represent SEM. Scale bars, 250 μm.



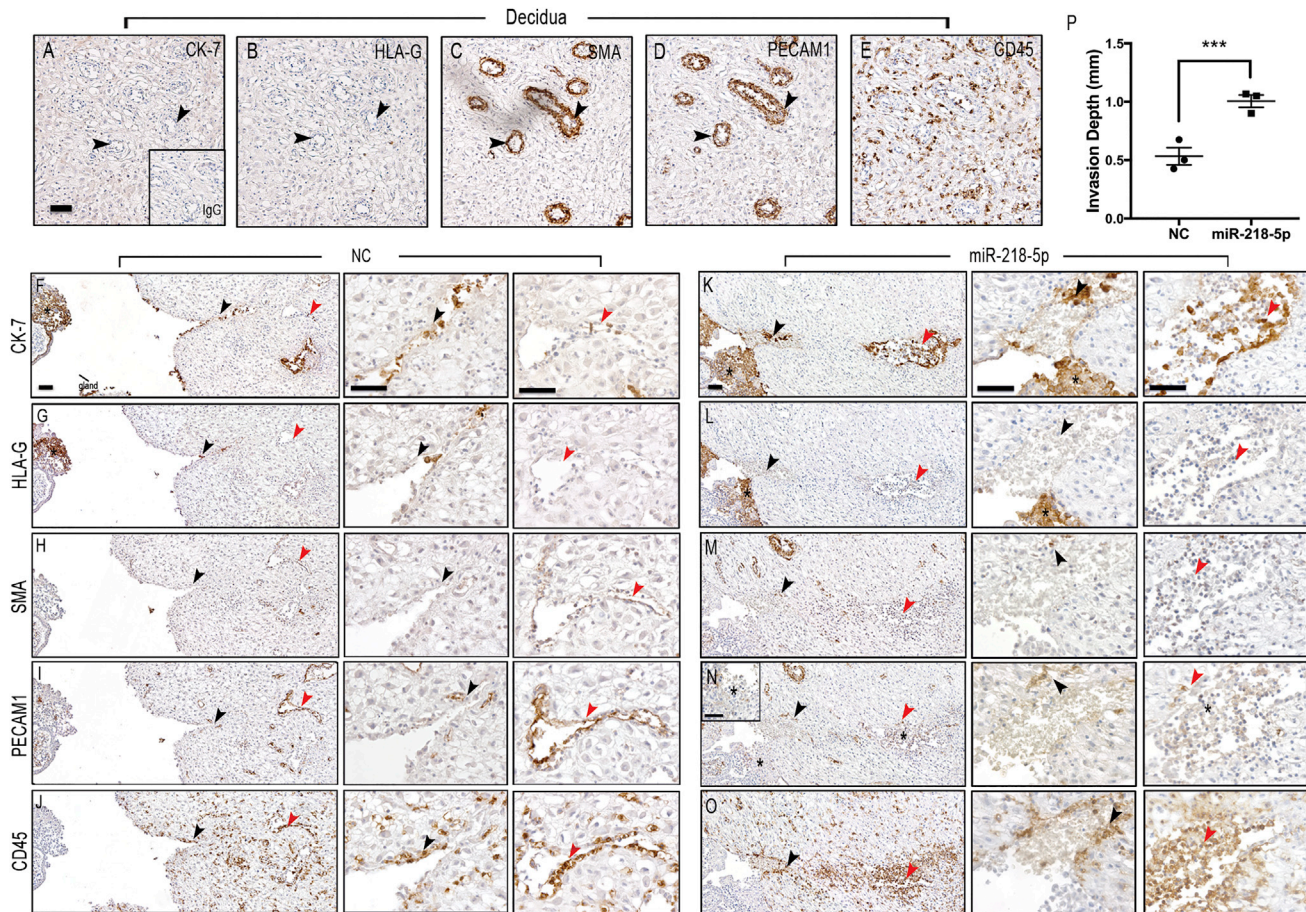


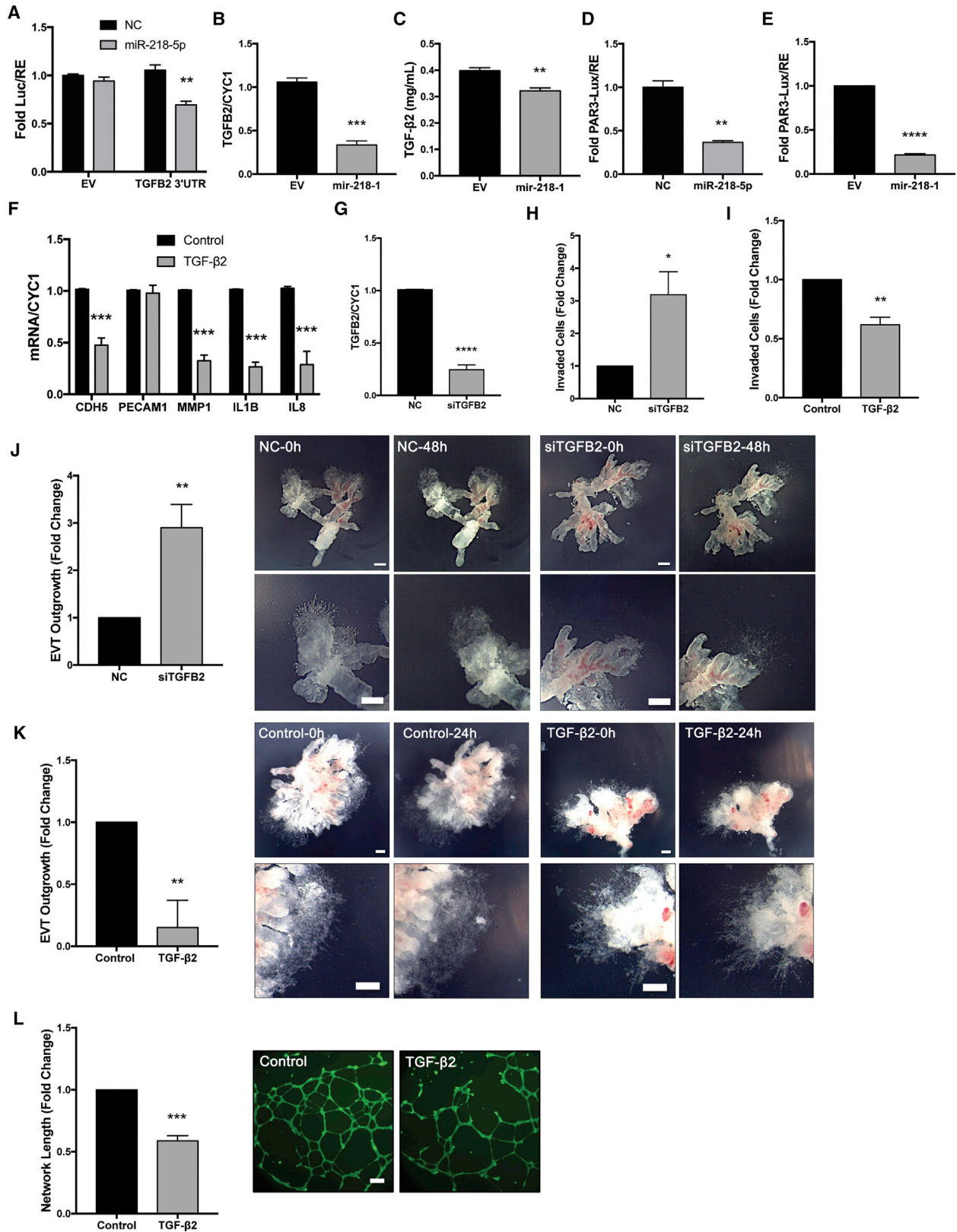
### Figure 5. miR-218-5p Accelerates Spiral Artery Remodeling

(A–E) Investigation of markers for trophoblasts (CK-7 and HLA-G), spiral arteries (SMA and PECAM1), and leukocytes (CD45) in *decidua parietalis* cultured alone. The tissue was negative for CK-7 and HLA-G (A and B, black arrowheads). Tight, non-invaded arterioles stained positive for SMA and PECAM1 (C and D, black arrowheads). Lymphocytes positive for CD45 were spread evenly throughout the tissue (E). (F–J) Placenta tissue pre-treated with NC was assessed for the degree of vessel remodeling. EVT's positive for CK-7 (F) and HLA-G (G) (black asterisks, \*) entered the proximal arteriole (black arrowheads), and a few cells also reached the distal portion (red arrowheads). Smooth muscle (H) and endothelial (I) cells were mostly removed in the proximal portion (black arrowheads) of the spiral arteriole but remained intact in the distal portion (red arrowheads), suggesting that the vessel was at an early "active phase" of vascular transformation. Leukocyte recruitment (J) at the site of remodeling was observed (arrowheads). (K–O) Placenta tissue pre-treated with miR-218-5p showed an accelerated degree of vessel remodeling. CK7-positive (K) and HLA-G-positive (L) EVT's (black asterisks, \*) entered the proximal portion of the arteriole (black arrowheads) and invaded the distal portion (red arrowheads). Only a few cells positive for SMA (M) remained at the proximal (black arrowheads) but also the distal (red arrowheads) portions of the arteriole. Smooth muscle cells in both proximal (black arrowheads) and distal portions had been predominantly removed, and cells in the lumen showed signs of phagocytosis (red arrowheads). Only residual PECAM1-positive endothelial cells (N) remained at both the proximal (black arrowheads) and distal (red arrowheads) portions of arteriole. EVT's were weakly positive for PECAM1 in the placenta column and the endovascular EVT's at the distal site of remodeling (black asterisks, \*). Extensive recruitment of leukocytes to the site of active remodeling (arrowheads) and associated clearing of leukocytes from surrounding tissue was observed (O). (P) Quantification of the remodeling arterioles showed a doubling in depth of trophoblast invasion and vessel remodeling in miR-218-5p-pretreated placentas compared with the control (n = 3 independent experiments with 2–3 co-cultures per experiment). Error bars represent SEM. Scale bars, 50  $\mu$ m.

that transient transfection of miR-218-5p (Figure 6D) and stable transfection of mir-218-1 (Figure 6E) both significantly reduced SMAD transcriptional activity. Treatment with recombinant human TGF- $\beta$ 2 significantly decreased CDH5, MMP-1, IL-1B, and IL-8 mRNA levels, whereas PECAM1 was unaffected (Figure 6F). Silencing of TGF $\beta$ 2 by small interfering RNA (siRNA) (Figure 6G) resulted in a significant increase in invasion compared with the

scrambled siRNA control (Figure 6H). Conversely, treatment with TGF- $\beta$ 2 significantly decreased cell invasion (Figure 6I). First-trimester placenta explants treated with TGF $\beta$ 2 siRNA had a significantly larger EVT outgrowth area (Figure 6J), whereas TGF- $\beta$ 2 treatment had the opposite effect (Figure 6K). Furthermore, TGF- $\beta$ 2 decreased the ability of HTR8/SVneo cells to form a network-like structure (Figure 6L). Finally, in the placenta-decidual co-culture





(legend on next page)

experiments, we observed lower TGFB2 immunoreactivity in EVT columns of miR-218-5p-treated placental explants ones treated with NC (Figure S10).

To determine whether the effects of miR-218-5p on enEVT differentiation were mediated by TGF- $\beta$ 2, rescue experiments were performed. Control and miR-218-1 cells were treated with and without TGF- $\beta$ 2. We found that miR-218-1-induced MMP-1, CDH5, IL-1B and IL-8 expression was blocked by TGF- $\beta$ 2 (Figure 7A). TGF- $\beta$ 2 also reversed the pro-invasive phenotype observed in miR-218-1 cells (Figure 7B). Finally, the significantly larger network formed by miR-218-1 cells when seeded on Matrigel was lost after TGF- $\beta$ 2 treatment (Figure 7C).

## DISCUSSION

The precise mechanisms underlying the development of PE are still elusive. Although it is clear that there is a complex interplay of both placental and maternal factors, there is consensus that a disruption in the invasive trophoblast pathway is an important contributing factor to the etiology. Histological studies of PE tissues have consistently shown superficial EVT invasion, absence of enEVT differentiation, and consequent insufficient remodeling of maternal spiral arteries.<sup>36–38</sup> The mechanism of enEVT differentiation and spiral artery remodeling has not been well studied. In this study, we demonstrate that miR-218-5p induces trophoblast invasion, promotes EVT-to-enEVT differentiation, and accelerates spiral artery remodeling. To the best of our knowledge, this is the first report of an miRNA implicated in enEVT differentiation and spiral artery remodeling.<sup>13</sup>

In this study, we first investigated the expression level of miR-218-5p in healthy placental tissues compared with PE placentas to identify its biological and pathological relevance. Consistent with previous reports,<sup>23,24</sup> we found that miR-218-5p is downregulated in placenta tissues from patients diagnosed with PE. To date, it has been established that the period of deep placental invasion and spiral artery remodeling in the first and early second trimester is of particular importance in the onset of PE.<sup>39</sup> Using qRT-PCR, we found that miR-218-5p expression spikes in the tips of placental explants from 8 to 11 weeks. These findings suggest that miR-218-5p is expressed in the placenta, especially in EVTs, and that it may play a role in regulating the establishment of the maternal fetal interface. However, the precise cellular

localization of miR-218-5p within the placenta requires further confirmation by *in situ* hybridization.

Next, we assessed the consequence of mir-218-1 overexpression in the well-established immortalized first-trimester trophoblast cell line HTR8/SVneo.<sup>40</sup> We observed that cells stably transfected with mir-218-1 displayed a spindly morphology and a more disorganized cytoskeletal structure characteristic of highly motile cells, higher mRNA levels of several genes known to be enEVT markers or associated with trophoblast invasion, an increase in cell invasion and endothelium-like network-formation, and a reduction in proliferation rate. These changes are consistent with differentiation toward an invasive enEVT pathway.<sup>41,42</sup> A recent cDNA microarray study compared gene expression patterns between HTR8/SVneo cells grown under standard or network-forming conditions. They reported that network-forming cells expressed genes associated with cytoskeleton organization, cell migration, and blood vessel development, whereas mitotic genes associated with proliferation were more highly expressed in cells grown under standard conditions. Interestingly, *SLIT2*, which houses the *MIR218-1* gene, was among the pro-angiogenic genes upregulated in network-forming cells.<sup>43</sup>

Several genes upregulated by miR-218-5p have been well documented in previous work as promoters of trophoblast invasiveness and markers of endovascular differentiation. CDH5 and IL-8 were the most congruent markers upregulated by miR-218-5p in both our cell and tissue models. Studies of feto-maternal interface sections showed that the upregulation of CDH5 in healthy tissue EVTs is absent in PE-affected tissues. They further demonstrated that CDH5 promotes primary CTB invasiveness in culture.<sup>37</sup> Likewise, IL-8 promotes primary CTB and HTR8/SVneo cell migration and invasion.<sup>44</sup> MMP-1 is one of the top upregulated markers in stable mir-218-1 cells. As a collagenase, MMP-1 is responsible for the degradation of collagen-rich extracellular matrices, such as those abundantly found in the decidua and the myometrium.<sup>45</sup> MMP-1 was reported to be the highest downregulated MMP in PE cases. Specifically, there is a clear reduction in the MMP-1<sup>+</sup> EVT population, suggesting its involvement in the reduced invasiveness observed in the pathophysiology of PE.<sup>46</sup> IL-1B was reported to directly promote the motility of first-trimester EVT<sup>47</sup> and to regulate the degree of their invasiveness.<sup>48</sup> Both PECAM1 and CDH5

### Figure 6. miR-218-5p Targets TGFB2

(A) Luciferase reporter assay. miR-218-5p reduced luciferase activity in cells transfected with the TGFB2 3' UTR reporter but not in cells transfected with the EV (n = 3). (B) TGFB2 mRNA was downregulated in mir-218-1 cells compared with the control (n = 3). (C) ELISA quantification of TGF- $\beta$ 2 showed a downregulation in the conditioned media collected from mir-218-1 stable cells compared with EV (n = 3). (D) Transient transfection of miR-218-5p reduced SMAD transcription activity, as measured using a SMAD response reporter, pAR3-lux (n = 3). (E) mir-218-1-overexpressing cells had lower SMAD-induced luciferase activity compared with control cells (n = 3). (F) Cells treated with recombinant human TGF- $\beta$ 2 (10 ng/mL) for 24 hr downregulated key markers of invasion and endovascular EVT differentiation (n = 3). (G) Validation of siRNA targeting TGFB2 (siTGFB2) (n = 3). (H) Silencing of *TGFB2* increased cell invasion (n = 3). (I) Treatment with TGF- $\beta$ 2 suppressed invasion (n = 3). (J) Silencing of *TGFB2* enhanced first-trimester placental explant outgrowth. Placental explants were treated with 200 nM siTGFB2 or NC for 48 hr (n = 4). (K) Treatment with TGF- $\beta$ 2 (10 ng/mL) for 24 hr inhibited placental explant outgrowth (n = 5). (L) TGF- $\beta$ 2 inhibits network formation. HTR8/SVneo cells pre-treated with TGF- $\beta$ 2 (10 ng/mL) showed decreased network structures on Matrigel compared with the control (n = 3). Statistical analysis was performed using a two-tailed unpaired t test or (F) multiple t tests corrected for multiple comparisons with the Holm-Sidak method. \*p < 0.05, \*\*p < 0.01, \*\*\*p < 0.001, \*\*\*\*p < 0.0001. Error bars represent SEM. Scale bars, 250  $\mu$ m.

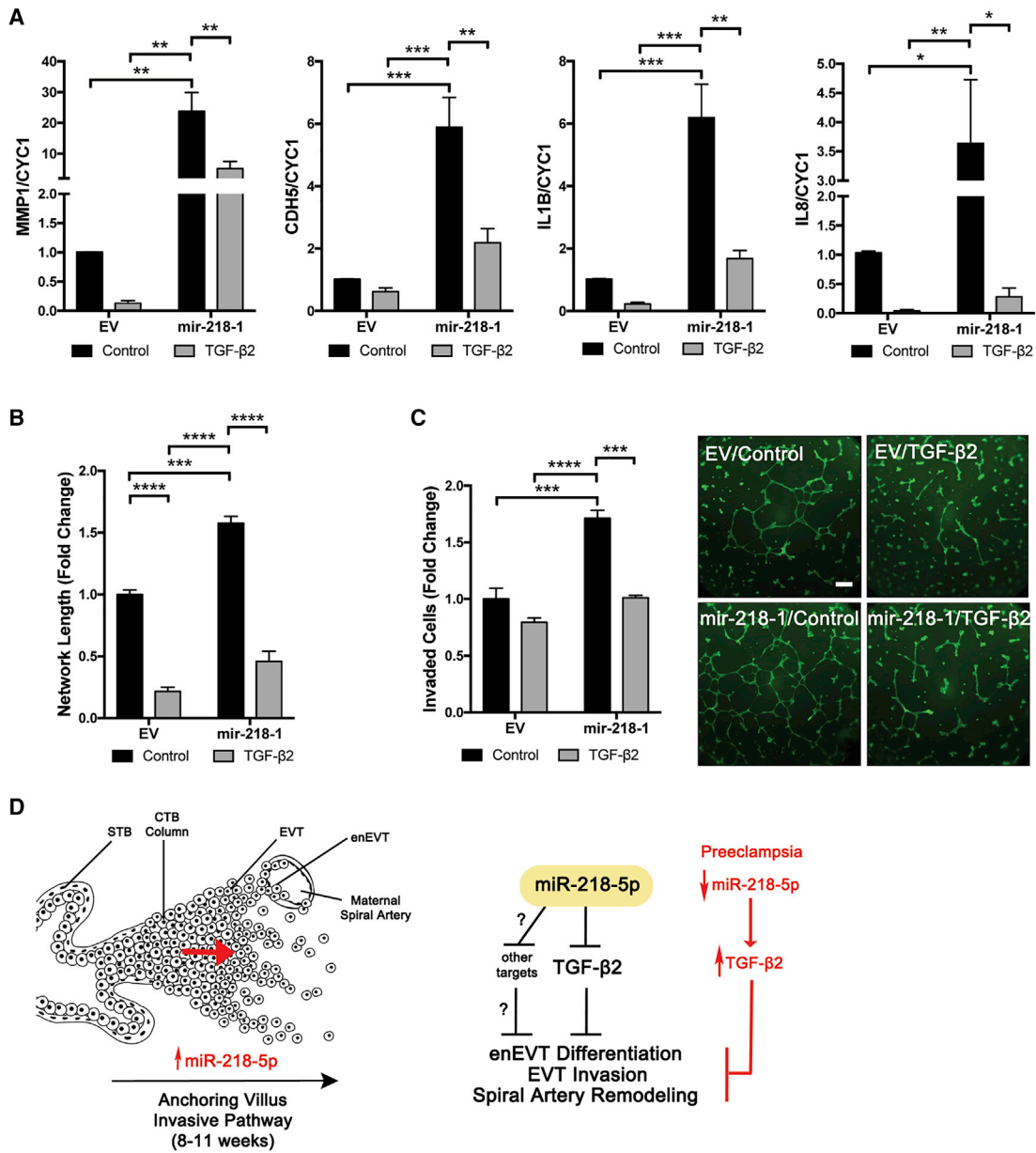


**Figure 7. miR-218-5p Exerts Its Effect through Suppression of TGF-β2**

(A) TGF-β2 reversed the effect of mir-218-1 on gene expression. EV control and mir-218-1-overexpressing stable cells were treated with TGF-β2 (10 ng/mL). mir-218-1 increased MMP-1, CDH5, IL-1B, and IL-8 mRNA levels, but these effects were abolished by TGF-β2. (B) TGF-β2 reversed the effect of mir-218-1 on cell invasion. Treatment with TGF-β2 inhibited the promoting effect of mir-218-1 on cell invasion. (C) TGF-β2 reversed the effect of mir-218-1 on network formation. TGF-β2 treatment reduced the ability of mir-218-1 stable cells to form network-like structures. (D) Proposed role of miR-218-5p in placental development and in the pathogenesis of preeclampsia. miR-218-5p is upregulated in EVTs to promote trophoblast invasion, endovascular differentiation, and spiral artery remodeling, in part through suppression of TGF-β2 signaling. Other target genes remain to be identified. Downregulation of miR-218-5p may lead to upregulation of TGF-β2 and other genes, which contributes to the shallow invasion of EVTs and defective spiral artery remodeling observed in PE placentas. STB, syncytiotrophoblast; CTB, cytotrophoblast; EVT, extravillous trophoblast; enEVT, endovascular EVT. \*p < 0.05, \*\*p < 0.01, \*\*\*p < 0.001, \*\*\*\*p < 0.0001. Error bars represent SEM. Scale bar, 500 μm.

were previously identified in EVTs at decidual-endothelial junctions, whereas CDH5 was shown to be essential in the transendothelial migration of enEVTs during spiral artery remodeling.<sup>49</sup> Similarly, both PECAM1 and CDH5 were found to be critical in

endothelial cell network formation on Matrigel.<sup>50</sup> Strong ECSCR immunoreactivity was detected in enEVTs of the placenta bed and within enEVTs of myometrial microvessels,<sup>51</sup> and ECSCR was strongly upregulated by mir-218-1 in our study.



Using an *ex vivo* model, we showed that placental explants pre-treated with miR-218-5p accelerated the decidual spiral artery remodeling process and induced PECAM1 expression in enEVTs in the vascular lumens. The remodeling of maternal spiral arteries is a complex multi-step process involving priming of the vessels by decidual immune cells and subsequent infiltration of enEVTs.<sup>52–54</sup> Our results suggest that miR-218-5p may upregulate genes involved in the epithelial-to-enEVT switch, resulting in an increased pool of enEVTs available for remodeling. The second mechanism responsible for the acceleration of spiral artery remodeling by miR-218-5p may lie in the upregulation of immune-responsive chemokines. Crosstalk between trophoblasts and the decidualized uterus is vital for establishment of a healthy fetomaternal interface. We found that decidua cocultured with miR-218-5p-treated placental explants showed an abundant recruitment of CD45-positive leukocytes to the site of vascular remodeling. Furthermore, treatment of placental explants with miR-218-5p upregulated the secretion of several pro-invasive and pro-angiogenic proteins into the conditioned medium. These data support a leukocyte chemotaxis effect of miR-218-5p-treated trophoblasts on the surrounding maternal tissue. Paracrine signals from the invading trophoblasts have been shown to contribute to the enriched cytokine milieu at the implantation site responsible for immune modulation and angiogenesis. In decidual stromal cells cultured in conditioned medium from primary first-trimester trophoblasts, CXCL1, IL-6, IL-8, and intercellular adhesion molecule-1 (ICAM1) are among the most highly upregulated genes.<sup>48</sup> EVT-derived IL-6 and IL-8 have been shown to act on endothelial cells in remodeling arterioles to produce CCL14 and CXCL6, which, in turn, recruit decidua natural killer cells (dNKs) and macrophages to the site of remodeling.<sup>55</sup> Likewise, trophoblast-secreted CXCL16 has been implicated in the recruitment of monocytes and T cells in first-trimester decidua.<sup>56</sup> Because miR-218-5p induced the expression and secretion of several cytokines and chemokines, notably CXCL1 and IL-8, it is possible that they are involved in miR-218-5p-promoted leukocyte recruitment. This possibility will be tested in the future.

Although the TGF- $\beta$  pathway has been implicated in placental development, its role in enEVT differentiation and spiral artery remodeling has not been reported. In this study, we show that miR-218-5p targets the TGFB2 3' UTR and downregulates TGFB2 mRNA levels and secretion. Furthermore, silencing of *TGFB2* mimicked some of the miR-218-5p phenotype. Specifically, in both HTR-8/SVneo cells and placental explants, we found that TGF- $\beta$ 2 inhibited invasion and EVT outgrowth, and incubation with TGF- $\beta$ 2 resulted in downregulation of enEVT markers in the trophoblast cell line. Moreover, high levels of miR-218-5p expression correlated well with low TGFB2 levels in EVTs during the most active phase of uteroplacental development. These findings suggest that TGF- $\beta$ 2 exerts a negative effect on enEVT differentiation and that its downregulation by miR-218-5p is in part responsible for the promotion of enEVT differentiation and spiral artery remodeling by miR-218-5p. The three TGF $\beta$  isoforms and their downstream regulatory molecules are located at the fetomaternal interface. The majority of studies suggest

that the TGF $\beta$  pathway is a negative regulator of trophoblast invasion.<sup>57–59</sup> Although the effect of TGF- $\beta$ 2 on the endovascular EVT pathway has not been previously reported, primary trophoblast treatment with TGF- $\beta$ 1 has been shown to downregulate CDH5.<sup>60</sup> Interestingly, miR-218-5p-treated placental explants also showed significant downregulation of the placenta-derived soluble TGF- $\beta$  co-receptor sEng, an anti-angiogenic protein known to be upregulated in sera of PE patients and to correlate with disease severity.<sup>61</sup>

In summary, this study provides the first evidence that miR-218-5p plays an important role in healthy placentation and may be involved in the pathogenesis of PE. Our findings suggest that miR-218-5p in the EVT population promotes the migration, invasion, and differentiation of enEVTs that contribute to proper remodeling of maternal spiral arteries, in part via inhibition of TGF- $\beta$ 2 signaling. Because miR-218-5p is downregulated in PE placentas, whereas serum TGF- $\beta$ 2 is upregulated in PE patients,<sup>62</sup> we propose that miR-218-5p is important in normal placenta development by limiting TGF- $\beta$ 2 signaling, and downregulation of miR-218-5p may contribute to the pathogenesis of PE (Figure 7D). Shallow EVT invasion and insufficient spiral artery remodeling are shared pathophysiologies of other pregnancy complications, such as intrauterine growth restriction (IUGR)<sup>63</sup> and pre-term labor.<sup>64</sup> Therefore, our findings regarding miR-218-5p may warrant further investigation into other gestational disorders. The use of miRNAs as potential plasma biomarkers has been investigated,<sup>28,65</sup> and the utility of miR-218-5p as both a predictive and prognostic marker in cancer has been suggested.<sup>66,67</sup> The possibility of using miR-218-5p as a biomarker of PE and possibly other disorders of pregnancy remains to be investigated. Furthermore, the use of miRNA-based therapeutic agents is a focus in next-generation medicine,<sup>68</sup> making miR-218-5p a great candidate for exploration in early PE intervention.

## MATERIALS AND METHODS

### Patients and Tissue Collection

Placental tissues from PE and healthy term controls were collected with informed consent from pregnant women who underwent perinatal medical care between 2010 and 2011 at the Department of Obstetrics and Gynecology, Peking University Third Hospital, China. The study protocol was approved by the Ethics Committee of the Institute of Zoology, Chinese Academy of Science. Specifically, 15 unique placenta samples were used for each group. Exclusion and diagnostic criteria can be found in the [Supplemental Materials and Methods](#), and the clinical characteristics of patients are listed in [Table S1A](#).

Additional fresh and frozen normal human tissues in this study were collected with informed consent through the BioBank program at the Research Centre for Women's and Infants' Health at Mount Sinai Hospital using a protocol approved by the Mount Sinai Hospital Research Ethics Board. For the evaluation of miR-218-5p expression across gestation, 69 placentas were used. Specifically, 13 first-trimester (5–12 weeks), 9 from second-trimester (13–20 weeks), 23 pre-term (26–36 weeks), and 24 term (37–40 weeks) placentas were

analyzed. Exclusion and diagnostic criteria can be found in the [Supplemental Materials and Methods](#), and the clinical characteristics of patients are listed in [Table S1B](#). To evaluate the endogenous level of miR-218-5p in trophoblast subpopulations, placentas from 6–11 weeks of gestation were carefully dissected into EVT columns, tips of villi beneath the columns, and villous branches. Tissues were snap-frozen in liquid nitrogen and stored at  $-80^{\circ}\text{C}$  for further RNA extraction. At least three unique placentas were dissected per gestational week.

### Cell Culture

An immortalized human first-trimester trophoblast cell line, HTR8/SVneo, was obtained from Dr. Charles Graham (Queen's University, Kingston, ON, Canada) and cultured as described previously.<sup>40</sup> Cells were periodically checked for mycoplasma contamination using the Mycoplasma Detection Kit QuickTest (BioTools, Jupiter, FL) and, when needed, treated with the MycoSmash Mycoplasma Removal Kit (BioTools) following the manufacturer's directions. All experiments were carried out on cells between passages 73 and 85.

### Transfections and Recombinant Protein Treatment

Transient transfection of siRNAs, miRNA mimics, or inhibitors (100 nM; sequences are listed in [Table S2](#)) was carried out using Lipofectamine RNAiMax (Thermo Fisher Scientific, Burlington, ON, Canada). Plasmid DNA was transfected into cells using Lipofectamine 2000 (Thermo Fisher Scientific). All transfections were performed in 6-well plates on 70% confluent cultures using 2  $\mu\text{L}$  of Lipofectamine reagent in Opti-MEM medium (Thermo Fisher Scientific). Transfections were carried out for 5 hr, and cells were then recovered in 10% fetal bovine serum (FBS)-containing medium for 16 hr. miR-218-5p, siTGFB2, and NCs were purchased from GenePharma (Shanghai, China). MirVana anti-miR-218-5p and a negative control were purchased from Thermo Fisher Scientific. Recombinant human TGF- $\beta$ 2 protein (Cedarlane, Burlington, ON, Canada) was used at 10 ng/mL in serum-free medium. To study the effect of TGF- $\beta$ 2 on enEVT marker expression, cells were treated with TGF- $\beta$ 2 for 24 hr. To determine whether TGF- $\beta$ 2 affects cell migration, invasion, and network formation, cells were pre-treated with TGF- $\beta$ 2 overnight prior to seeding for these assays.

### Generation of miR-218-1 Stable Cells

A portion of the *SLIT2* intron (NG\_047105; 281,231 to 281,568 bp) bracketing the miR-218-1 stem-loop sequence was amplified using the pair of primers listed in [Table S2](#) and cloned into a GFP-expressing pEGP-miR vector between the NheI and BamHI cut sites. HTR8/SVneo cells were subsequently transfected with the empty pEGP-miR vector or the miR-218-1 construct, followed by addition of 2  $\mu\text{g}/\text{mL}$  puromycin treatment for 2 weeks to select positive clones. All viable colonies were assessed for overexpression by detecting GFP signals and measuring miR-218-5p levels.

### RNA Extraction, Reverse Transcription, and Real-Time qPCR

Total RNA from cells and tissues was extracted using TRIzol reagent (Thermo Fisher Scientific) according to the manufacturer's protocol.

Reverse transcription was performed on 1.5  $\mu\text{g}$  total RNA with moloney murine leukemia virus reverse transcriptase (M-MuLV) (New England Biolabs, Whitby, ON, Canada). miRNA quantification was performed with the NCode miRNA First-Strand cDNA Synthesis Kit (Thermo Fisher Scientific), following the manufacturer's directions. Real-time qPCR was carried out with EvaGreen qPCR Master Mix (ABM, Richmond, BC, Canada), following the manufacturer's directions, on a RotorGene-Q thermocycler (Thermo Fisher Scientific). miR-218-5p levels were normalized to U6 small nuclear RNA (snRNA) levels, and all other genes were normalized to cytochrome c1 (CYC1). The relative mRNA level was calculated using the  $2^{-\Delta\Delta\text{ct}}$  method. Primer sequences are listed in [Table S2](#).

### Effects of miR-218-5p on enEVT Marker Gene Expression in Anchoring Villi

First-trimester placentas were collected as described above. Placental tissues between 8–10 weeks of gestation were dissected to collect EVT-containing villi. To assess changes in desired gene markers, the EVT-anchoring cell columns were carefully dissected with curved scissors and incubated with 200 nM of miR-218-5p, anti-miR-218-5p, or NC oligos in serum-free DMEM-F12 phenol red-free medium (Thermo Fisher Scientific) at  $37^{\circ}\text{C}$  with 3%  $\text{O}_2$  and 5%  $\text{CO}_2$ . For each treatment group within the experiment, approximately 50 EVT columns were used. After 48 hr, tissues were collected, snap-frozen in liquid nitrogen, and stored at  $-80^{\circ}\text{C}$  until RNA extraction. Because of limitations in tissue size, only one to two replicates were used per trial, and each experiment was repeated at least five times using different placentas.

### First-Trimester Human Placental Explant Culture

Placenta explant cultures were performed as described previously.<sup>27</sup> All successfully attached explants were randomly assigned to a treatment group. Explants were treated with NC, miR-218-5p, anti-miR-218-5p, or siTGFB2 ([Table S2](#)) at 200 nM or recombinant TGF- $\beta$ 2 at 10 ng/mL. Each treatment group had 3–5 replicates, depending on the availability of tissue. Each experiment was performed 4–5 times using different placentas. Explants were photographed immediately after adding treatment and subsequently at 24 and 48 hr using a Leica DFC400 camera attached to a dissecting microscope. ImageJ software (NIH, USA) was used to measure the area of EVT outgrowth. Specifically, total outgrowth area was calculated by subtracting the initial area before treatment from the area at the end of the treatment. To reduce quantification error, each explant replicate was quantified across all time points in one sitting. To reduce bias, the quantification was performed blindly when possible. At the end of the experiments, conditioned media were collected. Secreted chemokines were measured using the Bio-Plex Pro Human Chemokine Panel, 40-Plex panel (Bio-Rad).

### First-Trimester Placenta-Decidua Explant Co-culture

Placenta-decidua co-culture was performed as described previously.<sup>35</sup> Briefly, small sections of *decidua parietalis* and placental villi with EVT columns from the same patient were carefully dissected from tissues collected as described. Deciduae were placed at a  $45^{\circ}$  angle, epithelial side facing up, on Transwell inserts (EMD Millipore,

Toronto, ON, Canada) pre-coated with 120  $\mu$ L of undiluted phenol red-free Matrigel (BD Biosciences, Mississauga, ON, Canada). Placental explants were placed in serum-free medium containing 200 nM miR-218-5p or NC. Tissues were incubated at 37°C with 3% O<sub>2</sub> and 5% CO<sub>2</sub> for 24 hr. Treated placenta explants were washed five times in 1 $\times$  PBS to remove residual oligos. Villi were gently placed on the exposed epithelial surface of the decidua and, after 24 h, anchored with 50  $\mu$ L of Matrigel. Tissues were covered with serum-free DMEM-F12 medium supplemented with estradiol (0.3 ng/mL) and progesterone (20 ng/mL) and allowed to incubate for an additional 6 days, and then the tissues were fixed in 4% paraformaldehyde (Electron Microscopy Sciences, Hatfield, PA) for 1 hr. Tissues were dehydrated in ascending concentrations of ethanol, cleared in xylene, and embedded in paraffin. Blocks were sectioned to 5- $\mu$ m thickness and every tenth slide was histologically assessed by standard H&E staining. Decidua-alone samples served as a control to ensure that the selected tissue was not of *decidua basalis* origin. The experiment was performed on three individual placenta-decidua matched tissues. To quantify the extent to which spiral arteries were remodeled, serial sections of co-cultures, pretreated with NC or miR-218-5p and immunostained for SMA, were scanned (Visiopharm Integrator System version 3.0.8.0, Visiopharm, Horsholm, Denmark) at 100 $\times$ . Three measurements per explant were made (in millimeters) from the luminal epithelial surface of the decidua to the deepest point of vascular transformation, identified by loss of SMA staining, as reported previously.<sup>69</sup> Three independent experiments, each with 2-3 explants per group, were quantified.

#### Immunohistochemical Analysis

Immunohistochemical analysis was performed using the streptavidin peroxidase method as described previously.<sup>35</sup> Antigen retrieval for all antibodies used was performed by boiling slides in 10 mM sodium citrate. A blocking buffer of 10% goat serum and 2% rabbit serum (Dako, Burlington, ON, Canada) was used in a humidified chamber for 1 hr at room temperature, followed by overnight incubation at 4°C in primary antibody (Table S3). Incubation with mouse immunoglobulin G (IgG) (1:100, Dako) in place of primary antibody served as a negative control. Excess antibody was washed off, and subsequent incubations with anti-mouse or anti-rabbit biotinylated secondary antibody (1:300, Dako) and streptavidin-horseradish peroxidase (HRP)-conjugated tertiary reagent (Thermo Fisher Scientific) were performed for 1 hr each at room temperature. Specific signals were detected using a Dako 3,3'-diaminobenzidine (DAB) staining kit containing 0.02% H<sub>2</sub>O<sub>2</sub> and 0.075% 3,3'-diaminobenzidine in 1 $\times$  PBS. Slides were counterstained using Harris hematoxylin (1:2; Sigma-Aldrich, Oakville, ON, Canada), dehydrated in ascending series of ethanol, cleared in xylene, and mounted with Cytoseal (Thermo Fisher Scientific). Photographs were taken with an Olympus DP72 camera mounted on a BX61 Olympus microscope using the cellSens Standard program.

#### Reporter Constructs and Luciferase Assay

A luciferase reporter construct was generated by cloning a portion of the TGFB2 3' UTR containing the predicted miR-218-5p binding site

into the pMIR-REPORT (Thermo Fisher Scientific) vector downstream of a luciferase gene. The TGFB2 3' UTR was amplified from nucleotides 178 to 813 with the primers listed in Table S2. Luciferase assays were performed using the Dual-Luciferase Reporter Assay System according to the manufacturer's directions (Promega). A *Renilla* construct (10 ng/mL) was co-transfected with all experiments as a normalization control. TGF- $\beta$  signaling was assessed using the PAR3-Lux reporter and FAST2 as described previously.<sup>70</sup>

#### Isolation of HUVECs

Umbilical cords of term placentas were collected from Mackenzie Richmond Hill Hospital after cesarean delivery. The use of tissues was approved by the research ethics committee at Mackenzie Health and the York University Office of Research Ethics. All patients provided informed consent. HUVECs were isolated as described previously.<sup>71</sup> Cells were plated in M199 medium (Thermo Fisher Scientific) supplemented with 10% FBS, streptomycin (100  $\mu$ g/mL), penicillin (100 IU/mL), and 5 mg/mL endothelial cell growth supplement (BD Biosciences). Validation of isolated HUVECs was performed each time by examining the morphology and positive staining for vascular endothelial growth factor-A (VEGF-A) and PECAM1, and they were discarded after 10 passages.

#### Network Formation Assay and HUVEC Co-culture

On ice, 96-well plates were quickly coated with 50  $\mu$ L of Celtra Reduced Growth Factor BM Extract-PathClear (Trevigen, Gaithersburg, MD) and allowed to polymerize at 37°C for 30 min. For network formation assays, 25,000 HTR8/SVneo cells were seeded per well in 100  $\mu$ L of 10% FBS containing RPMI 1640. After 18 hr of culture, cells were stained with 1  $\mu$ M Calcein AM (Corning Life Sciences, Corning, NY) for 15 min, and pictures were taken at 20 $\times$  magnification on a fluorescence microscope. For co-culture assays, HUVECs and HTR8/SVneo cells were stained for 45 min with 1  $\mu$ M CellTracker Red CMTPX (Thermo Fisher Scientific) and CellTracker Green CMFDA (Sigma-Aldrich), respectively. When stained, cells were seeded at a one-to-one ratio with a total of 25,000 cells per well. Total network length was quantified in ImageJ using the NeuronJ plugin.<sup>72</sup> Each experimental group had a minimum of 3 replicates, and the experiment was repeated with at least three individual trials.

#### Statistical Analysis

Statistical analysis was performed using GraphPad Prism 7 ( $p < 0.05$ , 95% confidence interval). One-way ANOVA followed by Tukey's multiple comparisons test determined differences among several groups. Unpaired two-tailed Student's *t* test was used for comparisons between two groups. When test assumptions were not met, alternative statistical tests were used as necessary as specified in the corresponding figure legends.

Additional methods, including microarray analysis, cell proliferation, migration and invasion, LDH activity, ELISA, and detection of acetylated  $\alpha$ -tubulin by immunofluorescence can be found in the [Supplemental Materials and Methods](#).



## SUPPLEMENTAL INFORMATION

Supplemental Information includes Supplemental Materials and Methods, ten figures, and three tables and can be found with this article online at <https://doi.org/10.1016/j.ymthe.2018.07.009>.

## AUTHOR CONTRIBUTIONS

J.B. designed and performed most of the experiments, analyzed and interpreted data, and wrote the manuscript. C.D. lent her expertise in all tissue work and performed the bioplex assay. J. O., G.F., L.N., and M.S. carried out some cell experiments. C.D. J.O., G.F., and L.N. contributed to the interpretation of data and manuscript preparation. D.R., Y.L.W., and O.S. helped with tissue collection. I.Y., H.N., and S.J.L. provided guidance for study design and data interpretation. C.P. conceived the project, supervised the study, and edited the manuscript.

## ACKNOWLEDGMENTS

We thank Dr. Charles Graham for providing the HTR8/SVneo cells. We thank Dr. Jeff Wrana and Dr. Malcolm Whitman for providing the pAR3-Lux and FAST2 constructs, respectively. We thank the donors, RCWIH BioBank, the Lunenfeld-Tanenbaum Research Institute, the Mount Sinai Hospital/UHN Department of Obstetrics and Gynecology, Mackenzie Richmond Hill Hospital, and Peking University Third Hospital for the human specimens used in this study. This work was supported by grants from the Canadian Institutes of Health Research (MOP-81370, PJT-153146, and MOP-142730 to C.P. and CCI-92222 and CCI-132565 to C.P. and S.J.L.). J.B. was a recipient of Ontario Graduate Scholarships, the Queen Elizabeth II Graduate Scholarship in Science and Technology, and the Susan Mann Dissertation Scholarship from York University.

## REFERENCES

- Duley, L. (2009). The global impact of pre-eclampsia and eclampsia. *Semin. Perinatol.* 33, 130–137.
- Backes, C.H., Markham, K., Moorehead, P., Cordero, L., Nankervis, C.A., and Giannone, P.J. (2011). Maternal preeclampsia and neonatal outcomes. *J. Pregnancy* 2011, 214365–214367.
- Neiger, R. (2017). Long-Term Effects of Pregnancy Complications on Maternal Health: A Review. *J. Clin. Med.* 6, 76.
- Riise, H.K.R., Sulo, G., Tell, G.S., Iglund, J., Nygård, O., Vollset, S.E., Iversen, A.C., Austgulen, R., and Daltveit, A.K. (2017). Incident Coronary Heart Disease After Preeclampsia: Role of Reduced Fetal Growth, Preterm Delivery, and Parity. *J. Am. Heart Assoc.* 6, e004158.
- Davis, E.F., Lazdam, M., Lewandowski, A.J., Worton, S.A., Kelly, B., Kenworthy, Y., Adwani, S., Wilkinson, A.R., McCormick, K., Sargent, I., et al. (2012). Cardiovascular risk factors in children and young adults born to preeclamptic pregnancies: a systematic review. *Pediatrics* 129, e1552–e1561.
- Alsnes, I.V., Vatten, L.J., Fraser, A., Bjørngaard, J.H., Rich-Edwards, J., Romundstad, P.R., and Åsvold, B.O. (2017). Hypertension in Pregnancy and Offspring Cardiovascular Risk in Young Adulthood: Prospective and Sibling Studies in the HUNT Study (Nord-Trøndelag Health Study) in Norway. *Hypertension* 69, 591–598.
- Ji, L., Brkić, J., Liu, M., Fu, G., Peng, C., and Wang, Y.-L. (2013). Placental trophoblast cell differentiation: physiological regulation and pathological relevance to preeclampsia. *Mol. Aspects Med.* 34, 981–1023.
- Velicky, P., Knöfler, M., and Pollheimer, J. (2016). Function and control of human invasive trophoblast subtypes: Intrinsic vs. maternal control. *Cell Adhes. Migr.* 10, 154–162.
- Redman, C.W., Sargent, I.L., and Staff, A.C. (2014). IFPA Senior Award Lecture: making sense of pre-eclampsia - two placental causes of preeclampsia? *Placenta* 35 (Suppl), S20–S25.
- Chen, D.-B., and Wang, W. (2013). Human placental microRNAs and preeclampsia. *Biol. Reprod.* 88, 130.
- Doridot, L., Miralles, F., Barbaux, S., and Vaiman, D. (2013). Trophoblasts, invasion, and microRNA. *Front. Genet.* 4, 248.
- Hayder, H., O'Brien, J., Nadeem, U., and Peng, C. (2018). MicroRNAs: crucial regulators of placental development. *Reproduction* 155, R259–R271.
- McNally, R., Alqudah, A., Obradovic, D., and McClements, L. (2017). Elucidating the Pathogenesis of Pre-eclampsia Using In Vitro Models of Spiral Uterine Artery Remodelling. *Curr. Hypertens. Rep.* 19, 93.
- Small, E.M., Sutherland, L.B., Rajagopalan, K.N., Wang, S., and Olson, E.N. (2010). MicroRNA-218 regulates vascular patterning by modulation of Slit-Robo signaling. *Circ. Res.* 107, 1336–1344.
- Fish, J.E., Wythe, J.D., Xiao, T., Bruneau, B.G., Stainier, D.Y.R., Srivastava, D., and Woo, S. (2011). A Slit/miR-218/Robo regulatory loop is required during heart tube formation in zebrafish. *Development* 138, 1409–1419.
- Chiavacci, E., Dolfi, L., Verduci, L., Meghini, F., Gestri, G., Evangelista, A.M., Wilson, S.W., Cremisi, F., and Pitto, L. (2012). MicroRNA 218 mediates the effects of Tbx5a over-expression on zebrafish heart development. *PLoS One* 7, e50536.
- Amin, N.D., Bai, G., Klug, J.R., Bonanomi, D., Pankratz, M.T., Gifford, W.D., Hinckley, C.A., Sternfeld, M.J., Driscoll, S.P., Dominguez, B., et al. (2015). Loss of motoneuron-specific microRNA-218 causes systemic neuromuscular failure. *Science* 350, 1525–1529.
- Kong, Y., Sun, B., Han, Q., Han, S., Wang, Y., and Chen, Y. (2016). Retraction. *Int. J. Mol. Med.* 38, 1947.
- Liao, W.-X., Zhang, H.-H., Feng, L., Zheng, J., and Chen, D. (2008). Placental Expression of Slit/Robo Signaling: Implication in Angiogenesis and Preeclampsia. *Biol. Reprod.* 78, 126.
- Liao, W.-X., Laurent, L.C., Agent, S., Hodges, J., and Chen, D.-B. (2012). Human placental expression of SLIT/ROBO signaling cues: effects of preeclampsia and hypoxia. *Biol. Reprod.* 86, 111.
- Liao, W.-X., Wing, D.A., Geng, J.-G., and Chen, D.-B. (2010). Perspectives of SLIT/ROBO signaling in placental angiogenesis. *Histol. Histopathol.* 25, 1181–1190.
- Li, P., Peng, H., Lu, W.-H., Shuai, H.-L., Zha, Q.-B., Yeung, C.-K., Li, H., Wang, L.-J., Ho Lee, K.K., Zhu, W.J., and Yang, X. (2015). Role of Slit2/Robo1 in trophoblast invasion and vascular remodeling during ectopic tubal pregnancy. *Placenta* 36, 1087–1094.
- Xu, P., Zhao, Y., Liu, M., Wang, Y., Wang, H., Li, Y.-X., Zhu, X., Yao, Y., Wang, H., Qiao, J., et al. (2014). Variations of microRNAs in human placentas and plasma from preeclamptic pregnancy. *Hypertension* 63, 1276–1284.
- Zhu, X.-M., Han, T., Sargent, I.L., Yin, G.-W., and Yao, Y.-Q. (2009). Differential expression profile of microRNAs in human placentas from preeclamptic pregnancies vs normal pregnancies. *Am. J. Obstet. Gynecol.* 200, 661.e1–661.e7.
- Peng, C. (2003). The TGF-beta superfamily and its roles in the human ovary and placenta. *J. Obstet. Gynaecol. Can.* 25, 834–844.
- Hata, A., and Chen, Y.-G. (2016). TGF-β Signaling from Receptors to Smads. *Cold Spring Harb. Perspect. Biol.* 8, a022061.
- Nadeem, L., Munir, S., Fu, G., Dunk, C., Baczyk, D., Caniggia, I., Lye, S., and Peng, C. (2011). Nodal signals through activin receptor-like kinase 7 to inhibit trophoblast migration and invasion: implication in the pathogenesis of preeclampsia. *Am. J. Pathol.* 178, 1177–1189.
- Fu, G., Ye, G., Nadeem, L., Ji, L., Manchanda, T., Wang, Y., Zhao, Y., Qiao, J., Wang, Y.L., Lye, S., et al. (2013). MicroRNA-376c impairs transforming growth factor-β and nodal signaling to promote trophoblast cell proliferation and invasion. *Hypertension* 61, 864–872.
- Luo, L., Ye, G., Nadeem, L., Fu, G., Yang, B.B., Honarpour, E., Dunk, C., Lye, S., and Peng, C. (2012). MicroRNA-378a-5p promotes trophoblast cell survival, migration and invasion by targeting Nodal. *J. Cell Sci.* 125, 3124–3132.

30. Costa, M.A. (2016). The endocrine function of human placenta: an overview. *Reprod. Biomed. Online* 32, 14–43.
31. Tie, J., Pan, Y., Zhao, L., Wu, K., Liu, J., Sun, S., Guo, X., Wang, B., Gang, Y., Zhang, Y., et al. (2010). MiR-218 inhibits invasion and metastasis of gastric cancer by targeting the Robo1 receptor. *PLoS Genet.* 6, e1000879.
32. Cheng, Y., Yang, X., Deng, X., Zhang, X., Li, P., Tao, J., and Lu, Q. (2015). MicroRNA-218 inhibits bladder cancer cell proliferation, migration, and invasion by targeting BMI-1. *Tumour Biol.* 36, 8015–8023.
33. Jiang, Z., Song, Q., Zeng, R., Li, J., Li, J., Lin, X., Chen, X., Zhang, J., and Zheng, Y. (2016). MicroRNA-218 inhibits EMT, migration and invasion by targeting SFMBT1 and DCUN1D1 in cervical cancer. *Oncotarget* 7, 45622–45636.
34. Cartwright, J.E., Fraser, R., Leslie, K., Wallace, A.E., and James, J.L. (2010). Remodelling at the maternal-fetal interface: relevance to human pregnancy disorders. *Reproduction* 140, 803–813.
35. Dunk, C., Petkovic, L., Baczyk, D., Rossant, J., Winterhager, E., and Lye, S. (2003). A novel in vitro model of trophoblast-mediated decidual blood vessel remodeling. *Lab. Invest.* 83, 1821–1828.
36. Zhou, Y., Damsky, C.H., and Fisher, S.J. (1997). Preeclampsia is associated with failure of human cytotrophoblasts to mimic a vascular adhesion phenotype. One cause of defective endovascular invasion in this syndrome? *J. Clin. Invest.* 99, 2152–2164.
37. Zhou, Y., Fisher, S.J., Janatpour, M., Genbacev, O., Dejana, E., Wheelock, M., and Damsky, C.H. (1997). Human cytotrophoblasts adopt a vascular phenotype as they differentiate. A strategy for successful endovascular invasion? *J. Clin. Invest.* 99, 2139–2151.
38. Pijnenborg, R., Anthony, J., Davey, D.A., Rees, A., Tiltman, A., Vercruyse, L., and van Assche, A. (1991). Placental bed spiral arteries in the hypertensive disorders of pregnancy. *Br. J. Obstet. Gynaecol.* 98, 648–655.
39. Pijnenborg, R., Dixon, G., Robertson, W.B., and Brosens, I. (1980). Trophoblastic invasion of human decidua from 8 to 18 weeks of pregnancy. *Placenta* 1, 3–19.
40. Graham, C.H., Hawley, T.S., Hawley, R.G., MacDougall, J.R., Kerbel, R.S., Khoo, N., and Lala, P.K. (1993). Establishment and characterization of first trimester human trophoblast cells with extended lifespan. *Exp. Cell Res.* 206, 204–211.
41. Kemp, B., Kertschanska, S., Kadyrov, M., Rath, W., Kaufmann, P., and Huppertz, B. (2002). Invasive depth of extravillous trophoblast correlates with cellular phenotype: a comparison of intra- and extrauterine implantation sites. *Histochem. Cell Biol.* 117, 401–414.
42. Kaverina, I., and Straube, A. (2011). Regulation of cell migration by dynamic microtubules. *Semin. Cell Dev. Biol.* 22, 968–974.
43. Highet, A.R., Buckberry, S., Mayne, B.T., Khoda, S.M., Bianco-Miotto, T., and Roberts, C.T. (2016). First trimester trophoblasts forming endothelial-like tubes in vitro emulate a 'blood vessel development' gene expression profile. *Gene Expr. Patterns* 21, 103–110.
44. Jovanović, M., Stefanoska, I., Radojčić, L., and Vićovac, L. (2010). Interleukin-8 (CXCL8) stimulates trophoblast cell migration and invasion by increasing levels of matrix metalloproteinase (MMP)2 and MMP9 and integrins alpha5 and beta1. *Reproduction* 139, 789–798.
45. Sinai Talaulikar, V., Kronenberger, K., Bax, B.E., Moss, R., and Manyonda, I. (2014). Differences in collagen ultrastructure of human first trimester decidua basalis and parietalis: implications for trophoblastic invasion of the placental bed. *J. Obstet. Gynaecol. Res.* 40, 80–88.
46. Lian, I.A., Toft, J.H., Olsen, G.D., Langaas, M., Bjørge, L., Eide, I.P., Børndahl, P.E., and Austgulen, R. (2010). Matrix metalloproteinase 1 in pre-eclampsia and fetal growth restriction: reduced gene expression in decidual tissue and protein expression in extravillous trophoblasts. *Placenta* 31, 615–620.
47. Prutsch, N., Fock, V., Haslinger, P., Haider, S., Fiala, C., Pollheimer, J., and Knöfler, M. (2012). The role of interleukin-1 $\beta$  in human trophoblast motility. *Placenta* 33, 696–703.
48. Hess, A.P., Hamilton, A.E., Talbi, S., Dosiou, C., Nyegaard, M., Nayak, N., Genbecev-Krtolica, O., Mavrogianis, P., Ferrer, K., Kruessel, J., et al. (2007). Decidual stromal cell response to paracrine signals from the trophoblast: amplification of immune and angiogenic modulators. *Biol. Reprod.* 76, 102–117.
49. Bulla, R., Villa, A., Bossi, F., Cassetti, A., Radillo, O., Spessotto, P., De Seta, F., Guaschino, S., and Tedesco, F. (2005). VE-cadherin is a critical molecule for trophoblast-endothelial cell interaction in decidual spiral arteries. *Exp. Cell Res.* 303, 101–113.
50. Matsumura, T., Wolff, K., and Petzelbauer, P. (1997). Endothelial cell tube formation depends on cadherin 5 and CD31 interactions with filamentous actin. *J. Immunol.* 158, 3408–3416.
51. Kilari, S., Remadevi, I., Zhao, B., Pan, J., Miao, R., Ramchandran, R., North, P.E., You, M., Rahimi, N., and Wilkinson, G.A. (2013). Endothelial cell-specific chemotaxis receptor (ECSCR) enhances vascular endothelial growth factor (VEGF) receptor-2/kinase insert domain receptor (KDR) activation and promotes proteolysis of internalized KDR. *J. Biol. Chem.* 288, 10265–10274.
52. Craven, C.M., Morgan, T., and Ward, K. (1998). Decidual spiral artery remodelling begins before cellular interaction with cytotrophoblasts. *Placenta* 19, 241–252.
53. Harris, L.K. (2010). Review: Trophoblast-vascular cell interactions in early pregnancy: how to remodel a vessel. *Placenta* 31 (Suppl), S93–S98.
54. Smith, S.D., Dunk, C.E., Aplin, J.D., Harris, L.K., and Jones, R.L. (2009). Evidence for immune cell involvement in decidual spiral arteriole remodeling in early human pregnancy. *Am. J. Pathol.* 174, 1959–1971.
55. Choudhury, R.H., Dunk, C.E., Lye, S.J., Aplin, J.D., Harris, L.K., and Jones, R.L. (2017). Extravillous Trophoblast and Endothelial Cell Crosstalk Mediates Leukocyte Infiltration to the Early Remodeling Decidual Spiral Arteriole Wall. *J. Immunol.* 198, 4115–4128.
56. Huang, Y., Zhu, X.-Y., Du, M.-R., and Li, D.-J. (2008). Human trophoblasts recruited T lymphocytes and monocytes into decidua by secretion of chemokine CXCL16 and interaction with CXCR6 in the first-trimester pregnancy. *J. Immunol.* 180, 2367–2375.
57. Irving, J.A., and Lala, P.K. (1995). Functional role of cell surface integrins on human trophoblast cell migration: regulation by TGF- $\beta$ , IGF-II, and IGFBP-1. *Exp. Cell Res.* 217, 419–427.
58. Lash, G.E., Otun, H.A., Innes, B.A., Bulmer, J.N., Searle, R.F., and Robson, S.C. (2005). Inhibition of trophoblast cell invasion by TGFB1, 2, and 3 is associated with a decrease in active proteases. *Biol. Reprod.* 73, 374–381.
59. Prossler, J., Chen, Q., Chamley, L., and James, J.L. (2014). The relationship between TGF $\beta$ , low oxygen and the outgrowth of extravillous trophoblasts from anchoring villi during the first trimester of pregnancy. *Cytokine* 68, 9–15.
60. Cheng, J.-C., Chang, H.-M., and Leung, P.C.K. (2013). Transforming growth factor- $\beta$ 1 inhibits trophoblast cell invasion by inducing Snail-mediated down-regulation of vascular endothelial-cadherin protein. *J. Biol. Chem.* 288, 33181–33192.
61. Venkatesha, S., Toporsian, M., Lam, C., Hanai, J., Mammoto, T., Kim, Y.M., Bdoah, Y., Lim, K.H., Yuan, H.T., Libermann, T.A., et al. (2006). Soluble endoglin contributes to the pathogenesis of preeclampsia. *Nat. Med.* 12, 642–649.
62. Shaarawy, M., El Meleigy, M., and Rasheed, K. (2001). Maternal serum transforming growth factor beta-2 in preeclampsia and eclampsia, a potential biomarker for the assessment of disease severity and fetal outcome. *J. Soc. Gynecol. Investig.* 8, 27–31.
63. Lyall, F., Robson, S.C., and Bulmer, J.N. (2013). Spiral artery remodeling and trophoblast invasion in preeclampsia and fetal growth restriction: relationship to clinical outcome. *Hypertension* 62, 1046–1054.
64. Kelly, R., Holzman, C., Senagore, P., Wang, J., Tian, Y., Rahbar, M.H., and Chung, H. (2009). Placental vascular pathology findings and pathways to preterm delivery. *Am. J. Epidemiol.* 170, 148–158.
65. Li, Q., Long, A., Jiang, L., Cai, L., Xie, L.L., Gu, J., Chen, X., and Tan, L. (2015). Quantification of preeclampsia-related microRNAs in maternal serum. *Biomed. Rep.* 3, 792–796.
66. Jiang, Z., Song, Q., Yang, S., Zeng, R., Li, X., Jiang, C., Ding, W., Zhang, J., and Zheng, Y. (2015). Serum microRNA-218 is a potential biomarker for esophageal cancer. *Cancer Biomark.* 15, 381–389.
67. Cheng, M.-W., Wang, L.-L., and Hu, G.-Y. (2015). Expression of microRNA-218 and its clinicopathological and prognostic significance in human glioma cases. *Asian Pac. J. Cancer Prev.* 16, 1839–1843.

68. Chakraborty, C., Sharma, A.R., Sharma, G., Doss, C.G.P., and Lee, S.-S. (2017). Therapeutic miRNA and siRNA: Moving from Bench to Clinic as Next Generation Medicine. *Mol. Ther. Nucleic Acids* 8, 132–143.
69. Hazan, A.D., Smith, S.D., Jones, R.L., Whittle, W., Lye, S.J., and Dunk, C.E. (2010). Vascular-leukocyte interactions: mechanisms of human decidual spiral artery remodeling in vitro. *Am. J. Pathol.* 177, 1017–1030.
70. Wu, D., Luo, S., Wang, Y., Zhuang, L., Chen, Y., and Peng, C. (2001). Smads in human trophoblast cells: expression, regulation and role in TGF-beta-induced transcriptional activity. *Mol. Cell. Endocrinol.* 175, 111–121.
71. Crampton, S.P., Davis, J., and Hughes, C.C.W. (2007). Isolation of human umbilical vein endothelial cells (HUVEC). *J. Vis. Exp.* 2007, 183.
72. Meijering, E., Jacob, M., Sarria, J.-C.F., Steiner, P., Hirling, H., and Unser, M. (2004). Design and validation of a tool for neurite tracing and analysis in fluorescence microscopy images. *Cytometry A* 58, 167–176.